Comprehensive study of a detection mechanism and optimization strategies to improve sensitivity in a nanogap-embedded biotransistor

Sungho Kim,[1] Jae-Hyuk Ahn,[1] Tae Jung Park,[2] Sang Yup Lee,[2,3] and Yang-Kyu Choi[1,a)]
[1]*Department of Electrical Engineering, KAIST, Daejeon 305-701, South Korea*
[2]*BioProcess Engineering Research Center, Center for Systems and Synthetic Biotechnology, and Institute for the BioCentury, KAIST, Daejeon 305-701, South Korea*
[3]*Department of Bio & Brain Engineering, Department of Biological Sciences, and Bioinformatics Research Center, KAIST, Daejeon 305-701, South Korea*

(Received 1 April 2010; accepted 5 May 2010; published online 8 June 2010)

A novel biomolecular detection method, charge pumping, is investigated comprehensively as a biosensing mechanism. Tunneling electrons located in channel interface are responsible for a charge pumping current (I_{cp}) in a biosensing operation. The maximum tunneling distance (d_{tunnel}) of the electrons is the dominant factor to determine the amount of generated I_{cp}, which is closely correlated with the sensitivity in a proposed nanogap-embedded biotransistor structure. Using an analytical model in which biomolecules are considered as a trap-included insulator, the effects of the key parameters that govern d_{tunnel}, in this case the nanogap height, frequency of the applied pulse, and maximum pulse level, are analyzed. © *2010 American Institute of Physics*.
[doi:10.1063/1.3443580]

I. INTRODUCTION

Recently, due to their large surface-to-volume ratio,[1] field effect transistors (FET) based on silicon nanowires (Si NWs) or carbon nanotubes (CNTs) have shown extraordinary sensitivity for biosensing and have therefore attracted a considerable amount of attention.[2–5] The reported biosensing principle originates from the depletion or accumulation of a channel induced by the specific binding of charged biomolecules on the surface, which then affect the conductivity of the channel.[6]

Although Si NW FETs or CNT FETs have been demonstrated successfully in biosensor applications, their device geometries restrict the feasibility of a monolithic integration into conventional peripheral circuitry that consists of complementary metal oxide semiconductors (CMOS) for signal detection, processing, and transmission. Si NW or CNT FETs can be prepared through either a top-down or a bottom-up approach. For top-down approaches, advanced optical or electron-beam lithography tools should be employed to pattern the nanometer features.[7] Although it is compatible with conventional silicon technology, advanced lithography is costly. On the other hand, metal-catalytic growths for NWs (Ref. 8) or dispersed CNTs (Ref. 9) can be utilized as bottom-up approaches. However, these inevitably impose difficulty in positioning the device. These approaches are also associated with poor process compatibility.

To solve these problems, an alternative approach for the fabrication of a biosensor that utilizes the conventional FET structure directly has been proposed.[10,11] Throughout this process, no expensive lithography tools are needed for the definition of nanoscale patterns. However, their sensitivity levels are not comparable to NW-type biosensors, and their measured sensing signal typically shows severe data fluctuation. On the other hand, the authors in a previous work demonstrated a unique biomolecular detection method that was based on a charge pumping technique used with a nanogap-embedded conventional FET structure.[12,13] In the proposed technique, the trap density of the gate dielectric in a FET is introduced as a sensing parameter. When additional trap states are provided by biomolecules immobilized inside the nanogap carved by the partial etching of the gate dielectric, variation in the trap density results in a measurable change of the charge pumping current (I_{cp}). However, although the modulation of I_{cp} depended on the concentration of specific biomolecular bindings and could therefore serve as a sensing parameter for biosensors applications, a clear explanation of the mechanism and a physical analysis could not be provided at the time.

In the present study, a charge pumping method is investigated comprehensively for use as a biosensing mechanism. Using the analytical model and calculation, detailed mechanisms and optimization strategies to improve the level of sensitivity are presented.

II. EXPERIMENT

The proposed nanogap-embedded biotransistor (henceforth simply the biotransistor) device structure is based on a conventional n-channel FET, as shown in Fig. 1(a). A p-type silicon wafer was used as a substrate. For a gate insulator, 40 nm of SiO_2, corresponding to the nanogap height ($H_{\text{init,gap}}$) was thermally grown. N-type *in situ* doped polycrystalline silicon was deposited and patterned for a gate electrode. The source and drain were formed by ion-implantation and subsequent thermal activation. The gate insulator was then partially etched using a buffered oxide etchant to form the nanogap underneath the polysilicon gate. The length of the nanogap (L_{gap}) depended on the wet-etching time, which was

a)Author to whom correspondence should be addressed. Electronic mail: ykchoi@ee.kaist.ac.kr.

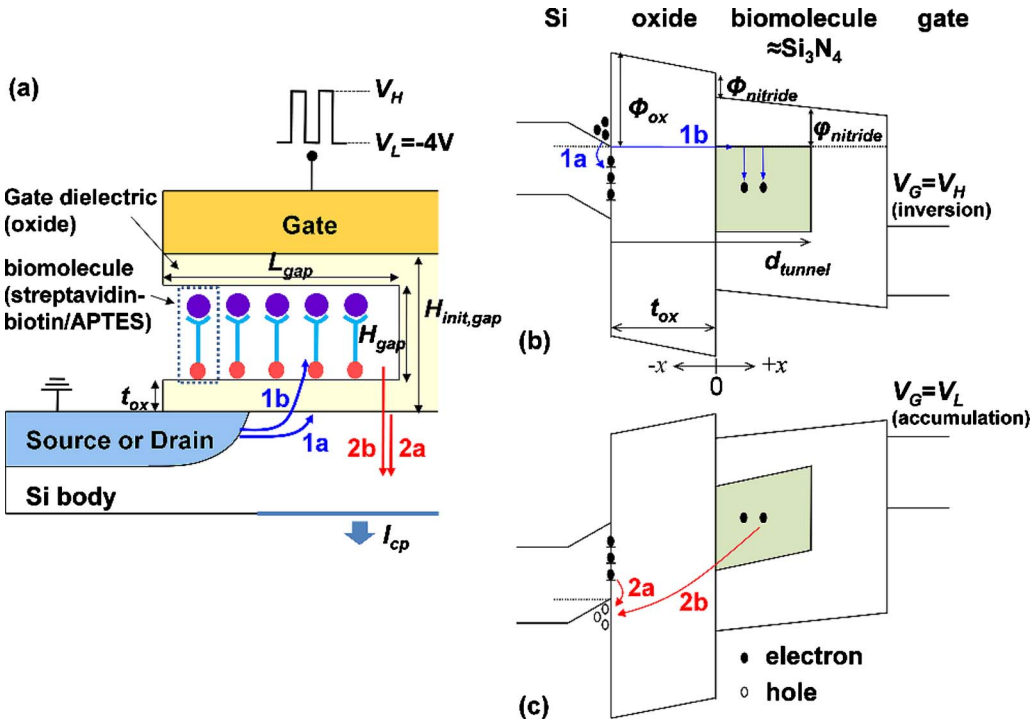

FIG. 1. (Color online) (a) Schematic diagram of the nanogap-embedded biotransistor and the experimental setup for the charge pumping measurements. (b) Schematic of the band diagram at the gate voltage of V_H and (c) at that of V_L. The shadowed area is the trap states in energy and space that will capture and hence contribute to I_{cp} during the charge pumping measurements.

fixed to 200 nm. Finally, a reoxidation process was carried out to form remaining oxide (t_{ox}), which was followed by annealing at 400 °C for 30 min with an ambient ratio of N_2:H_2=9:1. Actually, this remaining oxide cannot be perfectly removed because native oxide always forms on a silicon channel surface when the device is exposed to ambient air. Therefore, for good quality of the remaining oxide, the reoxidation and annealing process was additionally performed, and the effective nanogap height (H_{gap}) was defined. All measured biotransistors in these experiments had a gate length of 2 μm and a channel width of 20 μm.

For the measurement of I_{cp}, a pulse for charge pumping (f_{cp}) was applied into the gate electrode using a pulse generator. I_{cp} was then measured from the substrate using a semiconductor parameter analyzer with a grounded source and drain, as shown in Fig. 1(a). For the applied pulse wave form, whereas the pulse base level (minimum peak level of pulse, V_L) was fixed to −4 V, the maximum peak level of pulse (V_H) was varied (duty cycle=50%, rising and falling time=100 ns). When a pulse was applied into the gate electrode for charge pumping, the state of the transistor was then switched between the inversion mode by V_H and the accumulation mode by V_L repeatedly. Therefore, electrons trapped in the inversion mode recombined with holes from the substrate in the accumulation mode. This electron-hole recombination gave rise to a current flow from the substrate to the channel. This current is termed I_{cp}, and contains information pertaining to the trap properties in the gate dielectric.[14,15]

To bind the biotin-streptavidin specific binding on the nanogap surface, the immobilization of biotin on the nanogap surface was accomplished in a two-step procedure. The biotransistors were washed with an ethanol solution to remove contaminants and were then immersed in a 1% ethanol solution of 3-amonopropyltriethoxysilane (APTES) for 30 min. Subsequently, they were washed with pure ethanol and heated at 120 °C for 20 min. Sulfo-NHS-LC-biotin (10 mM) in 1×Phosphate buffered solution (PBS) solution (0.05% Tween 20) was then utilized in a 1 h reaction with the APTES-modified surface. The unreacted sulfo-NHS-LC-biotin was removed by deionized water (DW). Without a time delay, the biotinylated device was immersed into a streptavidin/PBS solution for another hour. This was followed by washing using DW and PBS.

III. RESULTS AND DISCUSSION

Figure 1(a) shows a schematic of the charge pumping measurement for biosensing. When V_H is applied to gate, the channel is inverted. Inversion electrons are then supplied by the source/drain contacts, and these electrons subsequently fill the traps near the channel [flow 1a in Figs. 1(a) and 1(b)]. Once the voltage switches from V_H to V_L, the channel accumulates excess holes that stem from the substrate terminal. For the trapped electrons (from the previous V_H step) near the channel, holes are captured from the valence band [flow 2a in Figs. 1(a) and 1(c)] and recombine with a previously captured electron, resulting in a positive current through the substrate terminal. This is the classical generation mechanism of I_{cp}. On the other hand, in the case of the proposed biotransistor, the biomolecules are not directly immobilized on the silicon channel but are instead immobilized on the regrown oxide, as shown in Fig. 1(a). Because the immobilized biomolecules are separated from the silicon channel

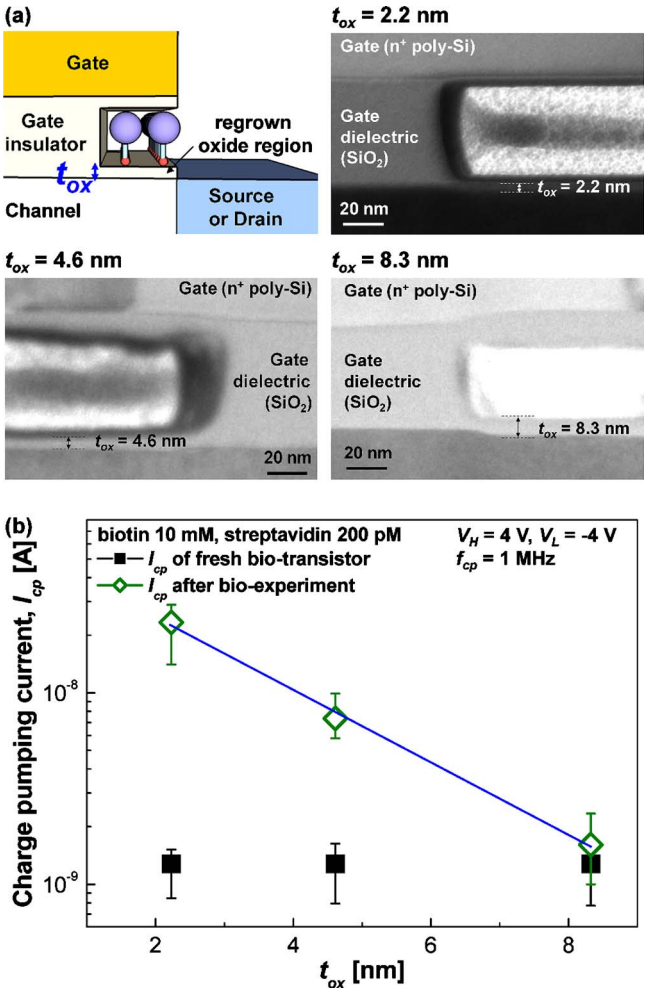

FIG. 2. (Color online) (a) Schematic diagram of the biotransistor after the bioexperiment along with TEM images of the nanogap that show different thicknesses of the regrown oxide (t_{ox}). (b) The relationship between the generated I_{cp} values and the location of the trap states from the channel. As t_{ox} increased, I_{cp} was reduced, although the number of trap states that stemmed from the biomolecules was identical among the three different t_{ox} cases.

due to the thickness of the regrown oxide (t_{ox}), classical mechanism for the generation of I_{cp} cannot properly explain the modulation of I_{cp} by biomolecules.

For the electrons and the traps in the biomolecules to interact with each other, the electrons should tunnel through the regrown oxide [flow 1b and 2b in Figs. 1(b) and 1(c)]. It was previously confirmed that the modulation of I_{cp} depended not on the regrown oxide but only on the concentration of specific biomolecular bindings.[12,13] Therefore, it can be understood that tunneling electrons located instead in the channel interface are the main contributor to the modulation of I_{cp} during the biosensing process, as the number of trap states in the regrown oxide is negligible compared to the number of biomolecules. Accordingly, to understand the biosensing mechanism in this biotransistor, the tunneling process of electrons during the charge pumping process should be considered. First, to investigate the relationship between the tunneling process and sensitivity experimentally, t_{ox} was intentionally controlled, as shown in Fig. 2(a). Figure 2(a) shows transmission electron microscope (TEM) images of the biotransistor. Using a reoxidation process controlled by a thermal oxidation process after the carving of the nanogap, t_{ox} was controlled at 2.2 nm, 4.6 nm, and 8.3 nm, respectively. Using these biotransistors with various t_{ox} values, the effects of different t_{ox} are represented in Fig. 2(b) when f_{cp} = 1 MHz. The initial amounts of generated I_{cp} are nearly equal in the three cases. However, although I_{cp} should be increased by the trap states additionally provided by the biomolecules after the bioexperiment, the increment of I_{cp} is reduced as t_{ox} is increased. This result implies that trap states far from the channel cannot contribute to the generation of I_{cp}, even with the high trap density provided by the biomolecules. Consequently, the tunneling process, especially maximum tunneling distance of electrons (d_{tunnel}) is the critical factor that governs the sensitivity of the biosensing process.

To develop an analytical model for a tunneling and trapping process in charge pumping, a biomolecule was considered as a trap-included insulator, as shown in Figs. 1(b) and 1(c). Because the electrical insulating properties of biomolecules, such as the permittivity, band gap, electron affinity, or trap distribution, are unknown, the physical parameters for modeling were obtained from silicon nitride, which is a well-known trap-included insulator.[16] Although the physical properties of silicon nitride may differ greatly from those of the biomolecules, even a simplified model can give valuable guideline to improve the sensitivity of the biotransistor. To calculate the tunneling probability of a channel electron, the potential barriers in the regrown oxide and the biomolecules can be obtained by [Fig. 1(b)],

$$V_{\text{oxide}}(x) = \phi_{ox} - qE_{ox}(x + t_{ox}) \quad \text{for} \quad -t_{ox} < x < 0,$$

$$V_{\text{bio}}(x) = \phi_{ox} - \phi_{\text{nitride}} - qE_{ox}t_{ox} - \frac{\varepsilon_{ox}qE_{ox}x}{\varepsilon_{\text{nitride}}} \quad \text{for} \quad x > 0,$$

where ϕ_{ox}=3.1 eV is the oxide barrier height for the electron injection,[17] ϕ_{nitride}=1.05 eV is the conduction-band offset of the oxide and silicon nitride,[17] q is the electron charge; ε_{ox} and $\varepsilon_{\text{nitride}}$ are the dielectric constants of the regrown oxide and the silicon nitride, respectively; and E_{ox} is the electrical field in the oxide and is a function of V_H. In addition, the trapping time constant, in other words the average time before an electron is trapped, is given by[15]

$$\tau_t = 1/(v_{th}\sigma_n n_s),$$

where n_s is the surface concentration of the electrons, v_{th} is the thermal velocity, and σ_n is the capture cross-section of the electrons. During the total tunneling time ($t=D/f_{cp}$, D is the duty cycle of the pulse), only tunneling electrons participate in the trapping process. Hence, the following applies:[18]

$$\text{tunneling probability of electron} = \frac{\text{trapping time constant}}{\text{total tunneling time}}.$$

Consequently, from the Wentzel–Kramers–Brillouin method,[17] the relationship between d_{tunnel} and the total tunneling time (t) can be obtained by

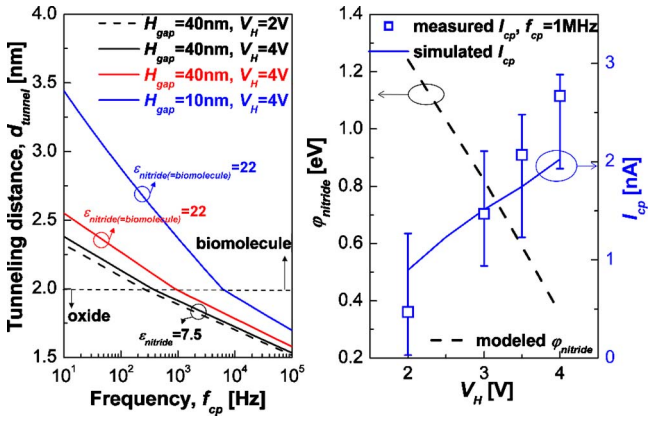

FIG. 3. (Color online) (a) Maximum electron tunneling distance as a function of f_{cp} for various values of V_H, H_{gap}, and $\varepsilon_{\text{nitride}}$. (b) The shallowest nitride-trap energy as a function of V_H.

$$\exp\left(-2\int_{-t_{ox}}^{d_{\text{tunnel}}}\frac{\sqrt{2m_{ox}V_{\text{oxide}}(x)}}{\hbar}dx\right) = \frac{1/(v_{th}\sigma_{\text{oxide}}n_s)}{D/f_{cp}} \quad \text{for} \quad -t_{ox} < d_{\text{tunnel}} < 0,$$

$$\exp\left(-2\int_{-t_{ox}}^{0}\frac{\sqrt{2m_{ox}V_{\text{oxide}}(x)}}{\hbar}dx - 2\int_{0}^{d_{\text{tunnel}}}\frac{\sqrt{2m_{\text{nitride}}V_{\text{nitride}}(x)}}{\hbar}\right) = \frac{1/(v_{th}\sigma_{\text{nitride}}n_s)}{D/f_{cp}} \quad \text{for} \quad d_{\text{tunnel}} > 0,$$

where n_s is the carrier density of the Si substrate extracted from a MEDICI simulator according to V_H, $v_{th}=10^7$ cm/s,[19] $\sigma_{\text{oxide}}=4\times10^{-16}$ cm^2,[15] and $\sigma_{\text{nitride}}=5\times10^{-13}$ cm^2.[19] $m_{ox}=0.5m_0$ and $m_{\text{nitride}}=0.5m_0$ are the effective masses in the oxide and silicon nitride,[17] respectively.

Based on equations developed above, d_{tunnel} can be calculated as a function of f_{cp} for various values of V_H, H_{gap}, and $\varepsilon_{\text{nitride}}$, as shown in Fig. 3(a) where t_{ox} is defined as 2 nm. It is shown in Fig. 3(a) that d_{tunnel} is increased when V_H is increased, because as a higher value of E_{ox} is applied to the regrown oxide (t_{ox}), the tunneling probability is increased. In addition, Fig. 3(b) shows the relationship between ϕ_{nitride} and V_H. ϕ_{nitride} is the shallowest trap energy at d_{tunnel}. As V_H is increased, ϕ_{nitride} is reduced, which implies that a wider energy level of the traps can contribute to the generation of I_{cp}. Thus, the increment in V_H can improve the sensitivity of biosensing in that more traps contribute to the generation of I_{cp} due to the increased value of d_{tunnel} and the range of trap energy levels. Figure 3(b) shows the measured and simulated I_{cp} values after the bioexperiment. The values exhibit consistency with aforementioned explanations. More I_{cp} was found with higher values of V_H; hence, higher sensitivity can be achieved by increasing V_H.

Another important parameter for increasing d_{tunnel} is f_{cp}. As shown in Fig. 3(a), d_{tunnel} is increased as f_{cp} is lowered. Essentially, I_{cp} is defined by $I_{cp}=f_{cp}Aq^2D_t\Delta\psi_s$ where $\Delta\psi_s$ is

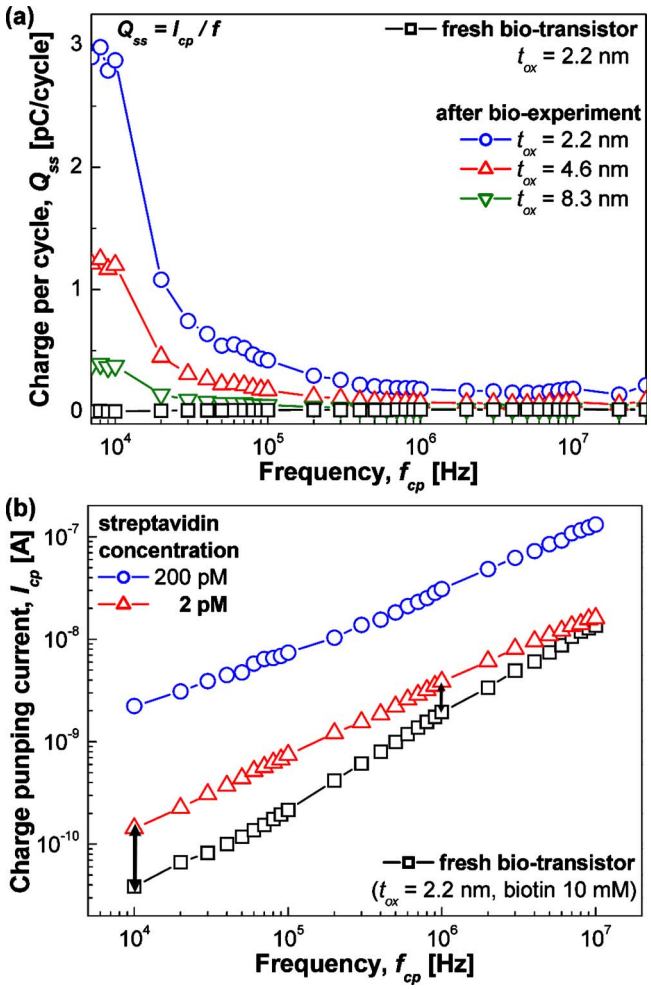

FIG. 4. (Color online) (a) Q_{ss} as a function of the frequency. In the high-frequency range, only traps near the channel interact with electrons in the channel. In contrast, in the low-frequency range, trap states located far from the channel can contribute to the generation of I_{cp} due to the tunneling process. (b) Measured I_{cp} values as a function of the frequency. The sensing margin is increased in the low-frequency range.

the change of the surface potential, D_t is the average trap density in energy, and A is the channel area.[15] When this equation is divided by f_{cp} on both sides, the new parameter (Q_{ss}, $Q_{ss}=I_{cp}/f_{cp}$) can be defined. Q_{ss} represents the amount of recombined charge per pulse cycle.[15] Given that Q_{ss} is independent of the frequency, the value of Q_{ss} should be constant for different pulse frequencies during the charge pumping process. Figure 4(a) shows the experimental results for Q_{ss} according to f_{cp}. With a fresh biotransistor, the value of Q_{ss} is mostly constant over all frequency ranges. After the bioexperiment, only a slight increase in Q_{ss} was observed in the high-frequency range because only trap states near the channel can interact with electrons flowing in the channel. In contrast, a sudden increase in Q_{ss} was observed in the low-frequency range because d_{tunnel} is increased due to the longer total tunneling time, allowing trap states far from the channel to contribute to the modulation of Q_{ss} and I_{cp}.[20,21] In addition, the increment in Q_{ss} is reduced as t_{ox} is increased. It is also understood that a greater values of t_{ox} reduces the probability that electrons will tunnel from the channel to the traps. These results assure that the sensitivity can be im-

proved if a lower pulse frequency is used during the charge pumping process. Figure 4(b) shows the measured values of I_{cp} as a function of f_{cp}. When 1 MHz of pulse is applied for charge pumping, the sensing margin cannot sufficiently detect 2 pM of streptavidin. This sensing margin can be improved if f_{cp} is lowered. This implies that the additional trap states inside the biomolecules contribute to the modulation of I_{cp} in the low-frequency range via the tunneling process of the electrons. Consequently, sensitivity can fall below the picomole concentration regime, even when the biotransistor has a microscaled device dimension.

IV. CONCLUSIONS

In summary, a biosensing mechanism of charge pumping in a nanogap-embedded biotransistor was investigated. Immobilized biomolecules in the nanogap region provide extra trap states, and this leads to the modulation of I_{cp}. Tunneling electrons located instead in the channel interface are responsible for I_{cp} in the biosensing process. When the frequency and the maximum level of the applied pulse were optimized by the development of an analytical model, the microsized biotransistor showed sensitivity that was comparable to a NW-type FET without a scaled dimension of the nanostructure. This makes the fabrication of low-cost and highly sensitivity biosensor applications feasible.

ACKNOWLEDGMENTS

This research was supported by a Grant No. 08K1401-00210 from the Center for Nanoscale Mechatronics & Manufacturing, one of the 21st Century Frontier Research Programs supported by the Korea Ministry of Education, Science and Technology (MEST). It was partially supported by the National Research and Development Program NRDP (Grant No. 2009-0065615) for the development of biomedical function monitoring biosensors, sponsored by the NRL program of KOSEF (Grant. No. R0A-2007-000-20028-0).

[1] Y. Chen, X. Wang, M. K. Hong, S. Erramilli, P. Mohanty, and C. Rosenberg, Appl. Phys. Lett. **91**, 243511 (2007).
[2] Y. Cui, Q. Wei, H. Park, and C. M. Lieber, Science **293**, 1289 (2001).
[3] N. Elfström, A. E. Karlstrom, and J. Linnros, Nano Lett. **8**, 945 (2008).
[4] A. Star, E. Tu, J. Niemann, J. P. Gabriel, S. Joiner, and C. Valcke, Proc. Natl. Acad. Sci. U.S.A. **103**, 921 (2006).
[5] G. Zheng, F. Patolsky, Y. Cui, W. U. Wang, and C. M. Lieber, Nat. Biotechnol. **23**, 1294 (2005).
[6] F. Patolsky, G. Zheng, and C. M. Lieber, Anal. Chem. **78**, 4260 (2006).
[7] Z. Li, Y. Chen, X. Li, T. I. Kamins, K. Nauka, and R. S. Williams, Nano Lett. **4**, 245 (2004).
[8] M. C. McAlpine, R. S. Friedman, S. Jin, K. H. Lin, W. U. Wang, and C. M. Lieber, Nano Lett. **3**, 1531 (2003).
[9] J. Wang and M. Musameh, Anal. Chem. **75**, 2075 (2003).
[10] P. Estrela and P. Migliorato, J. Mater. Chem. **17**, 219 (2007).
[11] H. Im, X. J. Haung, B. Gu, and Y.-K. Choi, Nat. Nanotechnol. **2**, 430 (2007).
[12] S. Kim, J.-H. Ahn, T. J. Park, S. Y. Lee, and Y.-K. Choi, Appl. Phys. Lett. **94**, 243903 (2009).
[13] S. Kim, J.-H. Ahn, T. J. Park, S. Y. Lee, and Y.-K. Choi, Appl. Phys. Lett. **96**, 053702 (2010).
[14] J. S. Brugler and P. G. A. Jespers, IEEE Trans. Electron Devices **16**, 297 (1969).
[15] G. Groeseneken, H. E. Maes, N. Beltran, and R. F. Keersmaecker, IEEE Trans. Electron Devices **31**, 42 (1984).
[16] K. A. Nasyrov, V. A. Gritsenko, M. K. Kim, H. S. Chae, S. D. Chae, W. I. Ryu, J. H. Sok, J. W. Lee, and B. M. Kim, IEEE Electron Device Lett. **23**, 336 (2002).
[17] S. M. Sze and K. K. Ng, *Physics of Semiconductor Devices* (Wiley, Hoboken, New Jersey, 2007).
[18] Y.-Y. Liao, S.-F. Horng, Y.-W. Chang, T.-C. Lu, K.-C. Chen, T. Wang, and C.-Y. Lu, IEEE Electron Device Lett. **28**, 828 (2007).
[19] S. H. Gu, C. W. Hsu, T. Wang, W. P. Lu, Y. H. J. Ku, and C. Y. Lu, IEEE Trans. Electron Devices **54**, 90 (2007).
[20] R. E. Paulsen, R. R. Siergiej, M. L. French, and M. H. White, IEEE Electron Device Lett. **13**, 627 (1992).
[21] R. E. Paulsen and M. H. White, IEEE Trans. Electron Devices **41**, 1213 (1994).